

Negative differential conductivity in quantum spin chains

Giuliano Benenti,^{1,2} Giulio Casati,^{1,2} Tomaž Prosen,³ and Davide Rossini⁴

¹*CNISM, CNR-INFM, and Center for Nonlinear and Complex Systems,
Università degli Studi dell'Insubria, Via Valleggio 11, 22100 Como, Italy*

²*Istituto Nazionale di Fisica Nucleare, Sezione di Milano, Via Celoria 16, 20133 Milano, Italy*

³*Physics Department, Faculty of Mathematics and Physics, University of Ljubljana, Ljubljana, Slovenia*

⁴*International School for Advanced Studies (SISSA), Via Beirut 2-4, I-34014 Trieste, Italy*

Quantum transport properties of low dimensional materials are currently an object of intensive theoretical and experimental research [1, 2, 3]. So far, most of theoretical studies concentrated on the close-to-equilibrium situation by using the linear response formalism, while almost nothing is known about the physics of such systems far from equilibrium. Here we propose a conceptually simple model of an anisotropic one-dimensional quantum Heisenberg spin-1/2 chain coupled to a pair of macroscopic magnets. We find a regime in which the spin current at small driving obeys Ohm's law, while for sufficiently strong driving it exhibits a significant negative differential conductivity, namely increasing the driving decreases the current. This phenomenon arises as an outcome of a beautiful interplay between coherent quantum dynamics of the spin chain and incoherent spin pumping. We believe that our results provide a new paradigm for the physics of open quantum many-body systems driven far from equilibrium.

Our system is constituted by N interacting quantum spins 1/2, whose dynamics is described by an XXZ Heisenberg exchange Hamiltonian:

$$\mathcal{H}_S = \sum_{k=1}^{N-1} \left[J_x (\sigma_k^x \sigma_{k+1}^x + \sigma_k^y \sigma_{k+1}^y) + J_z \sigma_k^z \sigma_{k+1}^z \right]; \quad (1)$$

here σ_k^α ($\alpha = x, y, z$) are the Pauli matrices of the k -th spin, and $\Delta \equiv J_z/J_x$ denotes the xz anisotropy. Both ends of the spin chain are coupled to magnetic baths, that is, to magnets acting as reservoirs for the magnetization [4]. Within the so-called Markovian approximation, which holds provided the bath relaxation time scales are much shorter than the time scales of interest for the system's dynamics, the time evolution of the system's state, which is described by a density matrix $\rho(t)$, follows the Lindblad master equation [5]:

$$\frac{\partial \rho}{\partial t} = -\frac{i}{\hbar} [\mathcal{H}_S, \rho] - \frac{1}{2} \sum_{m=1}^4 \{L_m^\dagger L_m, \rho\} + \sum_{m=1}^4 L_m \rho L_m^\dagger, \quad (2)$$

where

$$\begin{aligned} L_1 &= \sqrt{\Gamma \mu_L} \sigma_1^+, & L_2 &= \sqrt{\Gamma(1 - \mu_L)} \sigma_1^-, \\ L_3 &= \sqrt{\Gamma \mu_R} \sigma_N^+, & L_4 &= \sqrt{\Gamma(1 - \mu_R)} \sigma_N^- \end{aligned} \quad (3)$$

are four Lindblad operators, $\sigma_k^\pm = (\sigma_k^x \pm i\sigma_k^y)/2$ are the raising and lowering operators, while $[\cdot, \cdot]$ and $\{\cdot, \cdot\}$ denote the commutator and the anti-commutator, respectively. Hereafter we use dimensionless units, by setting $\hbar = 1$, $J_x = 1$. The Lindblad operators L_1, L_2 act on the leftmost spin of the chain ($k = 1$), while L_3, L_4 on the rightmost one ($k = N$). The dimensionless parameters Γ and μ_L (μ_R) play the role of the system-reservoir coupling strength and of a left (right) chemical potential, respectively. In other words, $2\mu_{L,R} - 1 \in [-1, 1]$ is the corresponding bath's magnetization per spin in dimensionless units. We choose a symmetric driving: $\mu_{L,R} = \frac{1}{2}(1 \mp \mu)$, so that $\mu \equiv \mu_R - \mu_L \in [0, 1]$ is a single parameter controlling the driving strength. When μ is small we are in the linear response regime, while in the limiting case $\mu = 1$ (corresponding to $\mu_L = 0, \mu_R = 1$) the left (right) bath only induces up-down (down-up) spin flips. This last case can be thought of as two spin-polarized chains coupled to the system. For instance, one could have two oppositely polarized ferromagnets for the left and the right baths.

We study the stationary spin current across the system, as explained in Methods section. Quite surprisingly, for an anisotropy $|\Delta| > 1$, the stationary spin current exhibits a *negative differential conductivity* (NDC) phenomenon, as shown in Fig. 1. Namely, in the linear response regime of small μ we find an Ohmic behaviour $\langle j \rangle \propto \mu/N$ of the spin current $\langle j \rangle$; the current reaches a maximum at a certain value μ^* , and, further increasing μ , it decreases, thus exhibiting a negative differential. At maximum driving strength $\mu = 1$, the current drops *exponentially* with N . While the small- μ Ohmic behaviour is consistent with recent linear response numerical results [6], the NDC effect is completely unexpected.

NDC is robust upon the variation of the number N of spins (Fig. 1) and of the system parameters Γ and Δ (Fig. 2) [7]. By increasing Γ over more than four orders of magnitude, from $\Gamma = 10^{-2}$ to $\Gamma = 3 \times 10^2$, we find [see Fig. 2a)] that the driving strength μ^* at which the current reaches its maximum shifts from $\mu^* \approx 0.9$ to $\mu^* \approx 0.3$, thus considerably reducing the range of validity of the linear response regime. The maximal current drop, measured by $\langle j \rangle_{\mu=\mu^*} - \langle j \rangle_{\mu=1}$, is obtained for $\Gamma \approx 5$ [see Fig. 2b)]. When $\Gamma \ll 1$ the “contact resistance” $1/\Gamma$ becomes large and the current is small for any value of μ . On the other hand, for $\Gamma \gg 1$ we are in the quantum Zeno regime [8], where the coupling to the reservoirs is

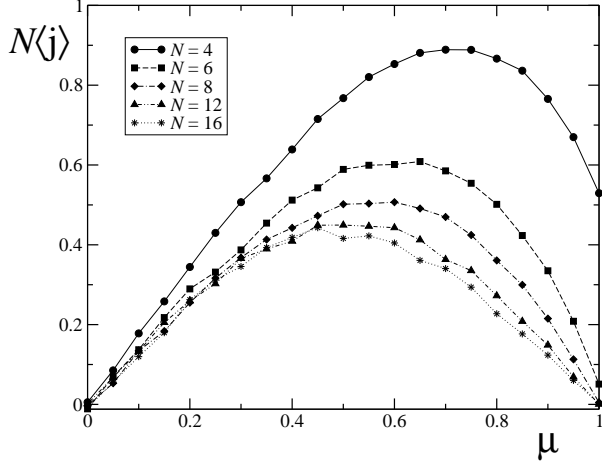


FIG. 1: Stationary spin current $\langle j \rangle$ as a function of the driving strength μ , with anisotropy $\Delta = 2$ and system-baths coupling strength $\Gamma = 4$. We rescaled the y -axis with the system size N in such a way that the small- μ Ohmic behaviour can be clearly appreciated.

strong and freezes the system's dynamics, thus drastically reducing the spin current.

In the bottom plots of Fig. 2, the driving strength μ^* and the current drop $\langle j \rangle_{\mu^*} - \langle j \rangle_1$ are shown as a function of the anisotropy Δ . For $|\Delta| < 1$ the negative differential conductivity effect is absent and the linear response regime $\langle j \rangle \propto \mu$ can be extended up to $\mu = 1$, with an ideally conducting behaviour, so that the spin current is independent of the system size [9]. On the other hand, NDC is observed at any $|\Delta| > 1$ [see Fig. 2c)]. Since spin transport along the chain is suppressed when $|\Delta| \gg 1$, there exists a value of the xz anisotropy, $|\Delta| \approx 1.5$ [see Fig. 2d)], at which the current drop is maximal. From the above analysis we infer that, for a chain of $N = 6$ spins, the optimal working point for the observation of the NDC phenomenon is $\Gamma \approx 5$, $|\Delta| \approx 1.5$.

Fig. 3 displays the stationary spin magnetization profiles $\langle \sigma_k^z \rangle_s$ along the chain, for the parameter values of Fig. 1. In the linear response regime, we observe a constant linear gradient, with the magnetizations $\langle \sigma_{1,N}^z \rangle_s$ of the two borderline spins close to the bath magnetizations $\langle \sigma_{L,R}^z \rangle = 2\mu_{L,R} - 1 = \mp\mu$. This behaviour is typical of normal Ohmic conductors [10]. Interestingly, in the limiting case $\mu = 1$ we notice the appearance of a stationary state characterized by two almost ferromagnetic domains, that are polarized as the nearest reservoir and whose *relative* width increases with the system size. These ferromagnetic regions are responsible for strongly inhibiting spin flips, and therefore for suppressing the spin current. We remark that we found no differences between a ferromagnetic ($J_z < 0$) and an antiferromagnetic ($J_z > 0$) spin coupling, and in particular we observed the same stationary spin profiles. While in the

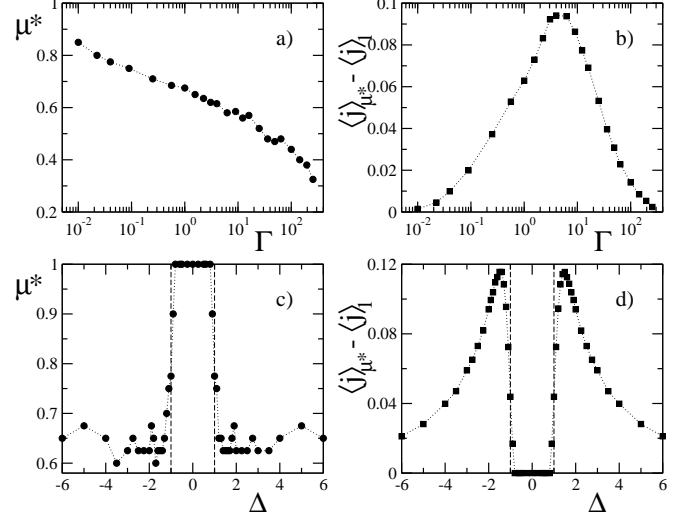


FIG. 2: Driving strength μ^* at which the spin current exhibits a maximum (left) and current at μ^* minus current at $\mu = 1$ (right), for a chain of $N = 6$ spins. Top panels are for $\Delta = 2$, bottom panels for $\Gamma = 4$.

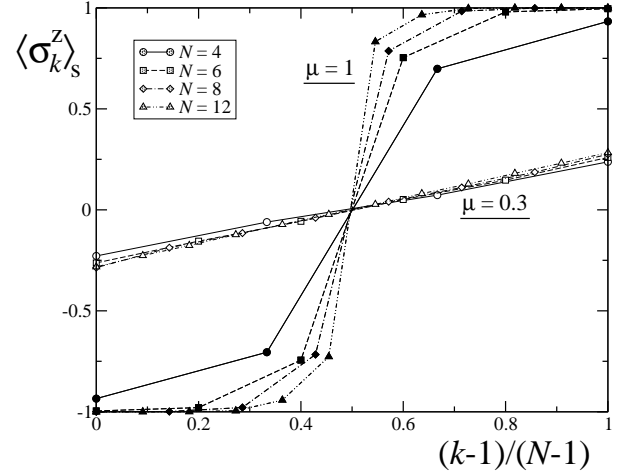


FIG. 3: Spin magnetization profiles $\langle \sigma_k^z \rangle_s$ versus the scaled spin index coordinate $\frac{k-1}{N-1}$ at $\Delta = 2$, $\Gamma = 4$, for driving strengths $\mu = 0.3$ (empty symbols) and $\mu = 1$ (filled symbols).

first case the formation of ferromagnetic domains may be somewhat intuitive, this is a priori not obvious for an antiferromagnetic coupling. Indeed in this last case, for the autonomous model (1), ferromagnetic domains correspond to a highly excited state; from the point of view of the Hamiltonian system, *the net effect of the baths is that of pumping energy into the system, while leading to a stationary state with very low entropy.*

As shown in Fig. 4, the time scale needed to reach the stationary state at $\mu = 1$ is exponentially long. This is the key observation on which our intuitive explanation of the NDC phenomenon relies, as we shall qualitatively ex-

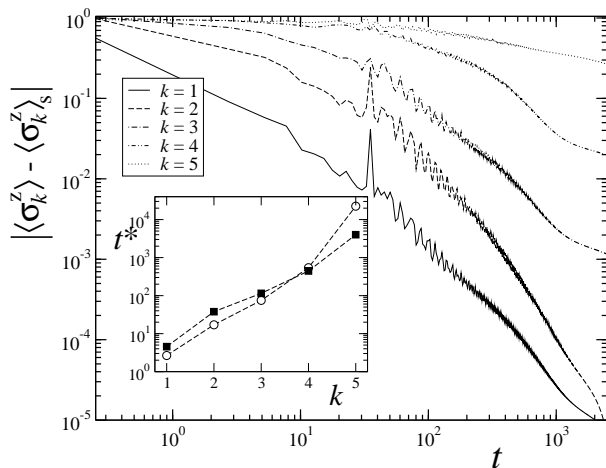


FIG. 4: Time approach to the equilibrium value of the spin magnetization of the leftmost spins, for $\mu = 1$, $N = 12$, $\Delta = 2$, $\Gamma = 4$. From bottom to top: $k = 1, 2, \dots, 5$. In the inset we plot the times t^* at which the magnetization reaches a given fraction of the corresponding stationary state value: $\langle \sigma_k^z \rangle = \frac{9}{10} \langle \sigma_k^z \rangle_s$, as a function of the spin index k (empty circles). The case with a single bath coupled to the first spin ($k = 1$) is also shown (filled squares).

plain below. Since at small μ the current grows linearly, it is sufficient to show that the current is suppressed in the limiting case $\mu = 1$ to conclude that, due to the continuity of $\langle j \rangle_\mu$, a region of negative differential conductivity exists. Therefore, we focus on the $\mu = 1$ case.

First, it is instructive to consider a situation in which the system is coupled to a single, fully polarized reservoir, $\mu_L = 0$. Regardless of the anisotropy Δ , the stationary state is pure and ferromagnetic, namely $|\downarrow\downarrow\cdots\downarrow\rangle$, since the Hamiltonian (1) conserves the overall magnetization while at the left boundary of the chain only the lowering operator $L_2 \propto \sigma_1^-$ acts. As Fig. 4 (inset) shows, at $|\Delta| > 1$ also for the single-bath case the convergence of $\langle \sigma_k^z \rangle$ to the equilibrium value $\langle \sigma_L^z \rangle = -1$ requires a time scale t^* which grows *exponentially* with the spin-bath distance k (this sharply contrasts with the ideally conducting case $|\Delta| < 1$, where t^* only grows *linearly* with k). Moreover, if an up-polarized reservoir is added at the right boundary, at $|\Delta| > 1$ the relaxation times t^* for the spins closer to the left than to the right boundary do not change significantly. This implies that, in our two-baths model, the spin polarization is practically affected only by the nearest bath.

The above results can be explained in terms of localization of one-magnon excitations. Given a ferromagnetic state $|0\rangle \equiv |\downarrow\downarrow\cdots\downarrow\rangle$, one-magnon excitations have the general form $\sum_{k=1}^N c_k |k\rangle$, where $|k\rangle = \sigma_k^+ |0\rangle$ describes the state with the k -th spin flipped. If the XXZ chain has open boundary conditions, there is an energy gap $2|J_z|$ between states $|1\rangle$ and $|N\rangle$ (spin-flip excitations at

the boundaries) and states $|2\rangle, |3\rangle, \dots, |N-1\rangle$. Since the coupling strength between $|k\rangle$ and $|k+1\rangle$ is $2|J_x|$, spin-flip excitations created at the border of the chain remain exponentially localized when $|J_z|/|J_x| = |\Delta| > 1$, over a localization length $\ell \sim 1/\ln|\Delta|$.

Consider now the action of the two baths. As can be clearly seen from Fig. 4, intermediate states in the relaxation to the stationary spin profile have two opposite-oriented ferromagnetic domains close to the baths. In order to enlarge them, spin-flip excitations should be propagated, through $\sigma_k^x \sigma_{k+1}^x$ and $\sigma_k^y \sigma_{k+1}^y$ exchange couplings of Hamiltonian (1), across the ferromagnetic domains to the chain boundaries. Suppose, for instance, that we have the leftmost m spins down and the $(m+1)$ -th spin up and that this excitation propagates to the left bath; then the bath can flip this spin down, thus ending up with a ferromagnetic domain with $m+1$ leftmost spins down. The crucial point is that the one-magnon propagation is exponentially localized at $|\Delta| > 1$. This explains why (i) equilibration needs exponentially long time scales and (ii) only the nearest bath is felt. We stress, however, that negative differential conductivity is observed after quite short time scales ($t \sim 10^2$), independently of the chain length. Indeed, it is sufficient to create a very small ferromagnetic region close to a bath, to strongly suppress current. For example, this *spin-blockade* mechanism can be clearly seen at $\mu \sim 0.9 - 0.95$, where asymptotically only a couple of outer spins reach magnetization values close to ± 1 , but still the current is far below the peak value at μ^* .

We mention that the presence of NDC is not related to integrability of the Heisenberg model. Indeed, we performed numerical simulations on XXZ chains in presence of a staggered magnetic field along the z direction, $B_{\text{stag}}(k) = (-1)^k B$. This system exhibits a transition from integrability to quantum chaos [11], when increasing the field strength B . We found that the NDC phenomenon is insensitive to such a transition.

Given the conceptual simplicity of the model, various experimental implementations could be envisaged. For instance, one could consider molecular spin wires [12, 13] with each boundary coupled to a magnetic impurity, where the desired populations $\{\mu_{L,R}, 1 - \mu_{L,R}\}$ of up/down spins can be pumped by means of electromagnetic fields. A completely different setup might be based on electronic transport through molecular wires that are embedded between two electrodes [14]. This is suggested by the fact that the XXZ chain can be mapped by the Jordan-Wigner transformation [15] into a tight-binding $t - V$ model of spinless fermions moving with a hopping amplitude $t = 2J_x$ on a N -site one-dimensional lattice, with nearest neighbour interaction of strength $V = 4J_z$. Here the spin current of the XXZ model becomes a charge current, the Lindblad operators (3) are mapped into operators injecting/extracting electrons at the lattice boundaries, and $\frac{1}{2}(1 + \langle \sigma_k^z \rangle)$ into the charge

density at site k . In particular, the ferromagnetic domains of Fig. 3 imply a *phase separation* in the fermionic model with all the electrons frozen in half of the lattice thus inhibiting charge transport, if $|V/t| > 2$, and, notably, irrespectively of whether the interaction is attractive or repulsive. Quite naturally, a NDC phenomenon similar to the one discussed in this paper is expected to take place for the heat current.

Methods. The time evolution of the master equation (2) has been numerically simulated by employing a Monte Carlo wave function approach, based on the technique of *quantum trajectories* [16]. The advantage of this approach is that, instead of storing and evolving a density matrix of size $2^N \times 2^N$, we work with a stochastically evolving state vector of size 2^N . The first two terms in the r.h.s. of Eq. (2) can be regarded as the evolution performed by an effective non-Hermitian Hamiltonian $\mathcal{H}_{\text{eff}} \equiv \mathcal{H}_S + i\mathcal{K}$, with $\mathcal{K} = -\frac{1}{2} \sum_m L_m^\dagger L_m$; the last term is responsible for the so-called quantum jumps, as explained below. If the initial density matrix describes a pure state $\rho(t_0) = |\phi(t_0)\rangle \langle \phi(t_0)|$, after a small amount of time dt it evolves into the statistical mixture

$$\rho(t_0 + dt) = \left(1 - \sum_m dp_m\right) |\phi_0\rangle \langle \phi_0| + \sum_m dp_m |\phi_m\rangle \langle \phi_m|, \quad (4)$$

where $dp_m = \langle \phi(t_0) | L_m^\dagger L_m | \phi(t_0) \rangle dt$ and the new states are defined by

$$|\phi_0\rangle = \frac{e^{-i\mathcal{H}_{\text{eff}}dt} |\phi(t_0)\rangle}{\sqrt{1 - \sum_m dp_m}}, \quad |\phi_m\rangle = \frac{L_m |\phi(t_0)\rangle}{\|L_m |\phi(t_0)\rangle\|}. \quad (5)$$

Therefore, with probability dp_m a jump to the state $|\phi_m\rangle$ occurs, while with probability $1 - \sum_m dp_m$ there are no jumps and the system evolves according to \mathcal{H}_{eff} .

In practice, we start from a pure random state $|\phi(t_0)\rangle$ and, at intervals dt much smaller than relevant dynamical time scales, we choose a random number $\varepsilon \in [0, 1]$. If $\varepsilon \leq \sum_m dp_m$, the state of the system jumps to one of the states $|\phi_m\rangle$ (to $|\phi_1\rangle$ if $0 \leq \varepsilon \leq dp_1$, to $|\phi_2\rangle$ if $dp_1 < \varepsilon \leq dp_1 + dp_2$, and so on). On the other hand, if $\varepsilon > \sum_m dp_m$ the evolution with the non-Hermitian Hamiltonian \mathcal{H}_{eff} takes place and we end up in the state $|\phi_0\rangle$. We repeat this process as many times as $n_{\text{steps}} = T/dt$, where T is the total evolution time. Assuming that there exists a single out-of-equilibrium steady state ρ_s , the expectation values $\langle A \rangle = \text{Tr}[A\rho_s]$ of any observable A (like the current j) is obtained after averaging in time $\langle \phi(t) | A | \phi(t) \rangle$ up to a long enough time T . For the sizes taken into account ($N \lesssim 16$), we checked that a good convergence for $\langle j \rangle$ is already reached at $T \sim 2 \times 10^4$, while longer integration times are needed in order to determine the stationary magnetization profiles at $\mu = 1$ ($T \sim 3 \times 10^5$ for $N = 12$ in Fig. 3). The non-Hermitian evolution of $e^{-i\mathcal{H}_{\text{eff}}dt}$ was simulated with a second order time Trotter expansion; a time slicing $dt \sim 2 \times 10^{-3}$ is sufficient to obtain accurate results.

The spin current $\langle j \rangle$ is calculated by looking at the left bath and summing up all up-down flips minus all down-up flips, and then dividing by the simulation time. Due to the conservation of the total magnetization in the Hamiltonian model (1), after the convergence time this current is precisely equal to the analogous quantity computed at the right bath and also equals the expectation value of $j_k = J_x(\sigma_k^x \sigma_{k+1}^y - \sigma_k^y \sigma_{k+1}^x)$ for any $k = 1, \dots, N-1$.

Acknowledgments. We thank M. Affronte, G. Falci, C. Hess and A. Parola for fruitful discussions. T.P. acknowledges support by grants P1-0044 and J1-7347 of Slovenian Research Agency.

-
- [1] Baeriswyl, D. & Degiorgi, L. (Eds.), *Strong Interactions in Low Dimensions*. (Kluwer Academic Publishers, Dordrecht, 2004).
 - [2] Žutić, I., Fabian, J. & Das Sarma, S. Spintronics: Fundamentals and applications. *Rev. Mod. Phys.* **76**, 323-410 (2004).
 - [3] Wolf, S.A. *et al.* Spintronics: A Spin-Based Electronics Vision for the Future. *Science* **294**, 1488-1495 (2001).
 - [4] Meier, F. & Loss, D. Magnetization Transport and Quantized Spin Conductance. *Phys. Rev. Lett.* **90**, 167204 (2003).
 - [5] Breuer, H.-P. & Petruccione, F. *The theory of open quantum systems* (Oxford University Press, Oxford, 2002).
 - [6] Prelovšek, P., El Shawish, S., Zotos, X. & Long, M. Anomalous scaling of conductivity in integrable fermion systems. *Phys. Rev. B* **70**, 205129 (2004).
 - [7] Furthermore, the phenomenon has been hinted by one of us in a different context of kicked open quantum dynamics: Prosen, T., unpublished notes available at [arXiv:0704.2252](https://arxiv.org/abs/0704.2252) [quant-ph].
 - [8] Facchi, P. & Pascazio, S. Quantum Zeno Subspaces. *Phys. Rev. Lett.* **89**, 080401 (2002).
 - [9] Zotos, X. Finite Temperature Drude Weight of the One-Dimensional Spin-1/2 Heisenberg Model. *Phys. Rev. Lett.* **82**, 1764-1767 (1999).
 - [10] Lepri, S., Livi, R. & Politi, A. Thermal conduction in classical low-dimensional lattices. *Phys. Rep.* **377**, 1-80 (2003).
 - [11] Haake, F. *Quantum Signatures of Chaos*, 2nd ed. (Springer, Berlin, 2001).
 - [12] Bogani, L. & Wernsdorfer, W. Molecular spintronics using single-molecule magnets. *Nature Mater.* **7**, 179-186 (2008).
 - [13] Ghirri, A. *et al.* Elementary excitations in antiferromagnetic Heisenberg spin segments. *Phys. Rev. B* **76**, 214405 (2007).
 - [14] Joachim, C., Gimzewski, J.K. & Aviram, A. Electronics using hybrid-molecular and mono-molecular devices. *Nature* **408**, 541-548 (2000).
 - [15] Mattis, D.C. *The Theory of Magnetism: An Introduction to the Study of Cooperative Phenomena* (Harper & Row, New York, 1965).
 - [16] Dalibard, J., Castin, Y. & Mølmer, K. Wave-Function Approach to Dissipative Processes in Quantum Optics. *Phys. Rev. Lett.* **68**, 580-583 (1992).